JOURNAL OF PROPULSION AND POWER
Vol. 14, No. 1, January–February 1998

Characterization of Fuel Regression in a Radial Flow Hybrid Rocket

J. R. Caravella Jr.,* S. D. Heister,† and E. J. Wernimont‡
Purdue University, West Lafayette, Indiana 47907

Reliable ignition and stable combustion have been achieved in a lab-scale radial-flow hybrid rocket engine. The device utilizes 85% hydrogen peroxide and polyethylene and was tested at chamber pressures ranging from 118 to 238 psia. Fuel regression behavior was characterized with respect to initial geometry and mass flux. The measured regression rates are greater than observed in axial port designs at the same flux and chamber pressure levels. Although the regression behavior is effected locally by the three-dimensional flow structure, the results were more uniform than predicted by lumped parameter ballistics approximations. For this reason, radial-flow designs with acceptable fuel utilization appear to be feasible.

Nomenclature

A_p = temporally averaged port area, in.^{2}
A_t = throat area, in.^{2}
c^* = characteristic exhaust velocity, ft/s
dt = incremental time, s
G = total mass flux, lbm/in.^{2} s
G_{ox} = oxidizer mass flux, lbm/in.^{2} s
g_c = gravitational constant, ft/s^2
h_i = initial gap height, in.
M = mass, lbm
$\dot{m}_{ox}$ = oxidizer mass flow rate, lbm/s
Nu = Nusselt number
OF = average mass oxidizer/fuel mixture ratio
P_c = head-end chamber pressure, psia
R = radial coordinate, in.
r = azimuthally averaged fuel regression rate, in./s
s = gap height, Fig. 2b
t_b = burning time, s
η_{c^*} = measured combustion efficiency

Subscripts
f = post-test condition
i = initial
th = theoretical value

Superscript
$-$ = radially weighted average quantity

Introduction

HYBRID rockets are currently being investigated because of interest in reducing cost and enhancing the safety and reliability of rocket propulsion systems. The conventional hybrid rocket employs a liquid oxidizer that is injected into a combustion chamber containing one or more fuel ports that run in a direction parallel to the centerline of the chamber. Because the fuel regression rate of typical hybrid propellant formulations is quite small (typically one-tenth that of a solid motor), large burn surface areas are required to generate high fuel flow rates and thrust levels. Therefore, numerous fuel ports are required to provide the necessary fuel surface area. This requirement not only increases the complexity of the fuel grain, but also reduces the volumetric efficiency of the combustion chamber (typical values can be as low as 50–60%).[1]

An interesting alternative, which may improve fuel section volumetric efficiency, is the radial flow hybrid rocket. Figure 1 highlights two of the numerous options afforded by this concept. In a radial flow engine, the fuel surfaces are oriented perpendicular to the centerline of the chamber (and the direction of thrust) to provide a large burn surface area. One can envision oxidizer injection in the center of this radial-flow configuration (Fig. 1a) or injection at the outer periphery of the fuel passage (Fig. 1b). Other possible configurations using multiple fuel plates, stacked on top of each other (with small gaps in between plates to maximize volumetric efficiency) can provide very large burn surface areas. Length-limited designs (such as upper-stage systems) and gas-generator/preburner appear as possible applications of this unique arrangement. In fact, preliminary design studies[2] indicate that the radial-flow arrangement can reduce the length of upper-stage propulsion systems by over 50%, as compared to current solid propulsion stages.

The center-injection concept in Fig. 1a has the advantage that the oxidizer injection is confined to a small region at the center of the chamber but has the disadvantage that an annular nozzle (or equivalent) is required. The annular-injection concept in Fig. 1b makes use of a conventional nozzle at the expense of a complex, annular injector. In this paper, we will concentrate our discussion and experiments on the center-injection radial flow hybrid rocket. The following section discusses some of the limited background material pertaining to this injection scheme and resulting flowfield. The subsequent sections discuss the experimental apparatus, test results, and conclusions from the study.

Background

To the authors' knowledge, there has been only one unpublished effort investigating any similar device. In the early 1990s, American Rocket Corporation (AMROC) tested a peripheral-injection design that utilized a single tangential injection element. The current effort presents the first work on axially fed center-injection radial flow hybrid rockets. Despite

Presented as Paper 96-3096 at the AIAA/ASME/SAE/ASEE 32nd Joint Propulsion Conference, Lake Buena Vista, FL, July 1–3, 1996; received July 25, 1996; revision received March 18, 1997; accepted for publication April 20, 1997.

*Graduate Research Assistant, School of Aeronautics and Astronautics; currently Staff Engineer, Boeing Defense and Space Group, Rocketdyne Division, 6633 Canoga Avenue, Canoga Park, CA 91303. Member AIAA.

†Associate Professor of Propulsion, School of Aeronautics and Astronautics, 1282 Grissom Hall. Member AIAA.

‡Graduate Research Assistant, School of Aeronautics and Astronautics; currently Lead Propulsion Engineer, Beal Aerospace, 15770 North Dallas Parkway, Suite 900, Dallas, TX 75248. Member AIAA.

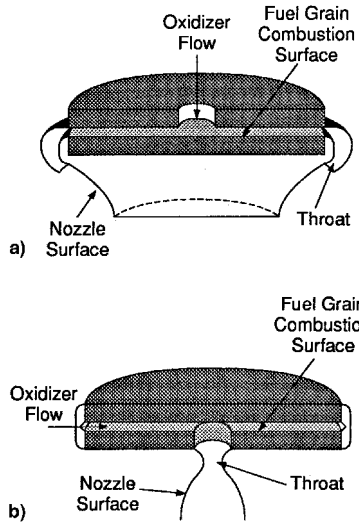

Fig. 1 Radial-flow hybrid rocket concepts.

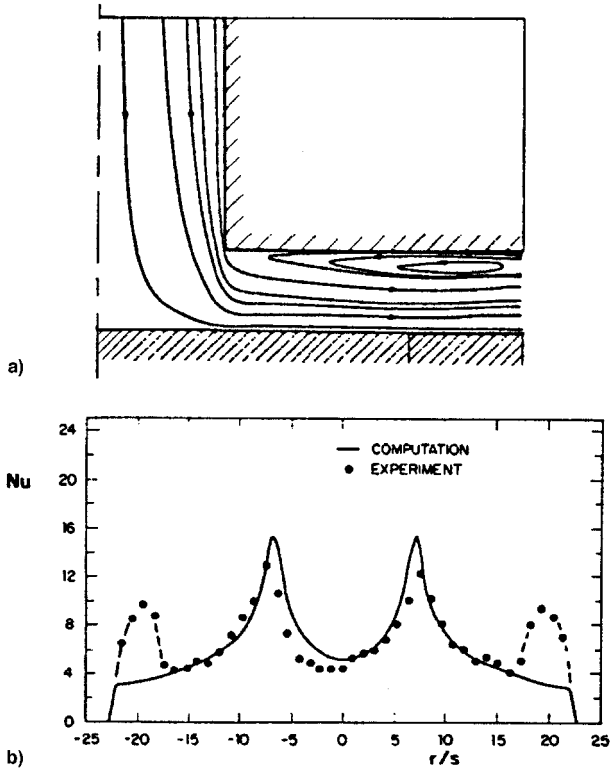

Fig. 2 Predicted streamline patterns and heat transfer on lower plate.[6]

the void in hybrid applications, several researchers have studied related radial flows with applications to centrifugal compressor diffusers and hydrostatic air bearings. Because the available flow area increases linearly with radial distance, basic momentum considerations dictate that an adverse pressure gradient must be present in most cases, and flow separation is a distinct possibility. In fact, researchers have observed (or calculated) flows in which both stationary[3–5] and oscillatory[6–8] separated regions exist.

For the experiments conducted in this study, a variation of the centered-injection geometry is used. An axial injector is located above the fuel disks, and the oxidizer impinges on the lower plate through a hole in the upper disk. Relevant experiments indicate a separated region attached to the inner corner of the upper plate. The streamline pattern associated with this flow (excerpted from calculations of Prata et al.[5]) is shown in Fig. 2a for an inlet Reynolds number based on a hydraulic diameter of 6.4×10^2. The Reynolds number based on the average hydraulic diameter, the velocity at the entry to the radial channel, and a viscosity based on the average OF ratio, varied between 2.7×10^4 and 6.6×10^4 in these experiments. Although we might expect a flowfield in general qualitative agreement with that of Fig. 2a, Reynolds number effects, mass addition, and changes in wall geometry with time (as a result of fuel consumption) can affect the character of the flow.

Prata et. al.[5] utilized napthalene sublimation to infer heat transfer rates in this region; sample results (with modeling predictions) are also shown in Fig. 2b for a Reynolds number of 4.3×10^2. The flowfield in the impingement region is similar to a round jet impinging on a plate; numerous studies have shown that peak heat transfer occurs near the edge of the jet because the center is presumably a stagnation region. The exact applicability of results such as these must be tempered by the fact that in a hybrid rocket, the fuel geometry in this region changes significantly with time.

Test Apparatus and Data Reduction Methodology

The primary goal of the experimental program was aimed at demonstrating ignition and stable combustion in a center-injection radial flow hybrid test article. A secondary goal involved characterization of the fuel regression behavior under a variety of different design and operating conditions. The experiments were performed at the Purdue University Rocket Propulsion Laboratory (PURPL), which houses a nitrogen gas-regulated facility designed for use with concentrated hydrogen peroxide with a capability of up to 400 psia chamber pressure.[10] Sacrificing thrust measurement, a vertical firing orientation was chosen to reduce the potential of liquid oxidizer pooling within the combustion chamber and to eliminate any gravity effects.

The geometry of the test article is shown in schematic form in Fig. 3. Using the catalytic decomposition ignition method employed by Wernimont and Heister[9] allowed work to begin immediately on the radial device. This set the oxidizer/fuel combination and the use of an axial injector for the current research. To accommodate the injection and ignition systems, a length of conventional single-port center-perforated fuel grain is used upstream of the radial flow combustion port. This fuel port is intended to completely sustain the decomposition of the incoming oxidizer spray to prevent any liquid oxidizer from pooling on the lower fuel disk. An annular throat was approximated by a finite number of conventional cylindrical throats distributed around the annulus. Seven throats were selected as a compromise between flange structural integrity, construction complexity, tangential flow instability considerations, and chamber pressure regressivity because of throat erosion.[2]

A digital data acquisition system was used to collect data on forward combustion chamber pressure and ullage pressure. Pressure transducers are mounted on the oxidizer tank and at the head end of the combustion chamber next to the injector. The system is run at 1250 Hz over four channels to yield an effective sampling rate of 312.5 Hz. All pressures are measured within $\pm 1\%$ accuracy. The oxidizer volumetric flow rate was calibrated from the pressure difference between the ullage tank and combustion chamber. Test parameters that can be varied are the initial combustion port gap height, oxidizer mass flow rate, corner geometry, burn time, and chamber pressure.

Other measurements include the dimensions and mass of all consumable components before and after firing, as well as the gap height between the fuel disks of the assembled rocket engine. Postfire measurements also include the thickness of the fuel disks at 260 different locations; 126 on the upper disk and 134 on the lower disk. The fuel disk thickness measurements were taken at 0.25-in.-radial increments on the 14 radial lines of symmetry based on nozzle location. A dial indicator on an extended set of jaws was used to manually measure the thick-

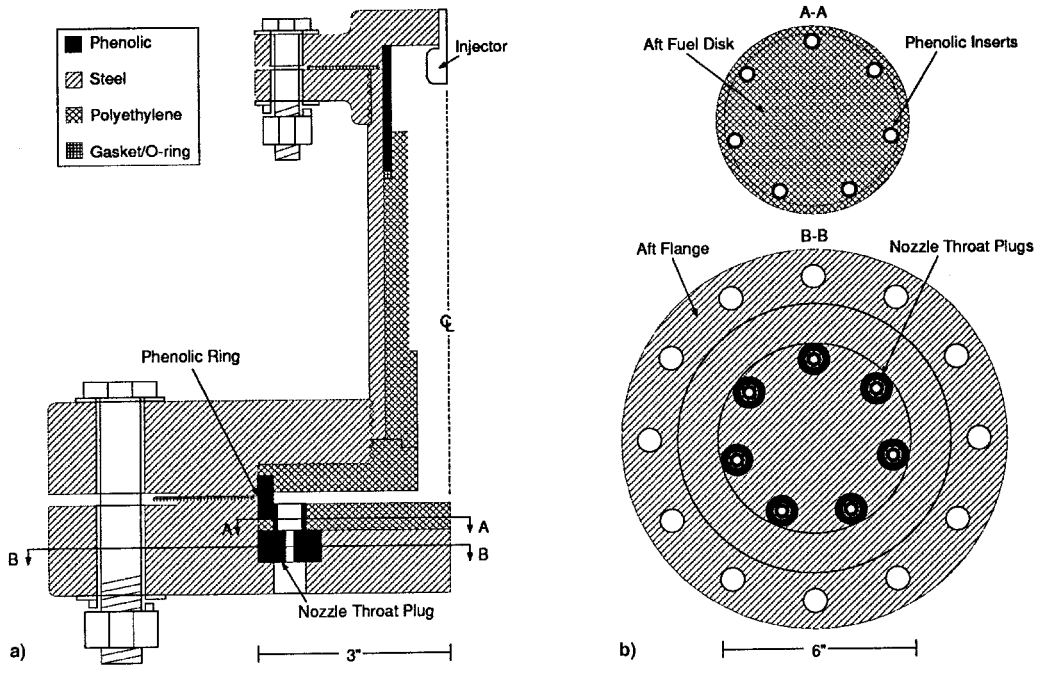

Fig. 3 Test engine design.

nesses to ±0.005 in. The radial and azimuthal locations were held roughly within 0.03 in. of their intended location.

The real time data were used to determine the oxidizer flow rate, which was then integrated to determine total oxidizer consumption. Chamber pressure data were integrated to determine average values for each test. The time-averaged OF ratio was calculated via

$$OF = \frac{\int_0^{t_b} \dot{m}_{ox}\, dt}{M_{f_i} - M_{f_f}} \tag{1}$$

where M_{f_i} and M_{f_f} are initial and final fuel masses, respectively. Theoretical characteristic velocity c^*_{th} was obtained from the NASA Lewis Research Center's One Dimensional Thermochemistry Code[10] at the average chamber pressure and OF values. The c^* combustion efficiency is calculated by

$$\eta_{c^*} = \frac{g_c \int_0^{t_b} P_c A_t\, dt}{c^*_{th}\left[\int_0^{t_b} \dot{m}_{ox}\, dt + (M_{f_i} - M_{f_f})\right]} \tag{2}$$

The preceding integrals were performed using trapezoidal integration, and burning times were measured from the initial chamber pressure rise to the beginning of tailoff.

The radial variation in regression rate was determined by azimuthally averaging the 14 regression rates calculated at each station. Average regression rate values for upper and lower plates ($\bar{r}_u$ and $\bar{r}_l$ in Table 1) are radial averages[2] of the azimuthally averaged data. While one must use caution in interpreting these averaged values, they were calculated to give the reader an estimate of the bulk regression rates achieved in these tests.

The accuracy in the regression rate, oxidizer mass flux, and total mass flux calculations were determined based on the nominal bias error in principal measurements of burn time, total expelled oxidizer mass, consumed fuel mass, radius, fuel grain thickness, and gap height. For a more detailed presentation of the error estimation method, see Ref. 2. Nominal bias error is estimated at 2% for burn time and twice that for total expelled oxidizer mass. This results in accuracy in a regression rate of 4%, an oxidizer mass flux of 5.9%, and in a total mass flux of 6% of nominal values.

Results

Initially, an exhaustive ignition test series (C1-a to C1-g, C2–C4) was performed beyond the worst-case test conditions expected to ensure safe ignition and testing. Initial tests (C1-a to C1-g) were conducted with only the nipple section and the upper fuel disk, while subsequent tests (C2) added the lower fuel disk but still omitted the throat plugs. This radial-exhaust test was run beyond the duration of the ignition system and actually choked the flow near the entrance to the radial flow section. Even in this extreme environment, the fuel grain remained lit. Both the C1 and C2 tests had a 45-deg bevel in the inlet of the upper fuel disk, after successfully firing C2, it was determined that this bevel was not needed to relieve the adverse pressure gradient because separation served as a beneficial flame holder. Test C3 and C4 had prototype fuel grain designs, but had extremely high nozzle erosion. The final nozzle design utilized silica phenolic material with the fiber layers oriented perpendicular to the flow.

The final nozzle material and fuel grain design were consistently applied to all remaining tests in the matrix shown in Table 1. Because the measured regression on early tests was higher than expected, the amount of oxidizer loaded was reduced and held fixed throughout the test series to minimize the chance of burn-through. This approach worked to an order of magnitude, but because relatively small amounts of fluid were loaded and some gets trapped in the feed lines, significant variation in actual expelled oxidizer was seen upon integration of the mass flow rate data. The loaded mass of oxidizer was maintained within ±0.5%, but the integrated expelled oxidizer mass differed by as much as 14% from the loaded mass.

The results of the parametric tests are summarized in Table 1. Test C5 is used as the baseline configuration, at a chamber pressure of 125 psi, a gap height of 0.2 in., an oxidizer mass flow rate of 0.16 lbm/s, and a burn time of roughly 10 s. To get an idea of how this device behaves with time, two more baseline configurations were fired at different burn times, tests C6 and C7. The effect of mass flux was investigated at a constant gap height by increasing the mass flow rate of the oxi-

Table 1 Summary of test conditions and results

Test index	h_i, in.	$\bar{m}_{ox}$, lbm/s	$\bar{P}_c$, psi	t_b, s	$\overline{OF}$	η_c^*	$\bar{G}_{ox}$, lbm/in.^{2} s	$\bar{G}$, lbm/in.^{2} s	$\bar{r}_{te}$, in./s	$\bar{r}_f$, in./s
C5	0.200	0.159	125.7	9.94	4.4	0.92	0.048	0.059	0.014	0.017
C6	0.200	0.169	119.0	13.38	4.7	0.83	0.045	0.055	0.013	0.017
C7	0.200	0.164	129.1	6.30	4.0	0.91	0.055	0.069	0.017	0.020
C8	0.200	0.245	130.5	6.80	4.9	0.91	0.077	0.092	0.018	0.021
C9	0.204	0.307	132.3	5.29	4.9	0.95	0.095	0.115	0.022	0.028
C10	0.306	0.246	126.7	7.05	5.1	0.89	0.058	0.070	0.016	0.022
C11	0.401	0.309	128.0	5.42	4.1	0.92	0.063	0.079	0.017	0.025
C12	0.405	0.171	118.6	10.73	4.8	0.85	0.033	0.040	0.010	0.016
C13	0.202	0.179	238.1	10.01	3.9	0.94	0.050	0.063	0.014	0.021
C14	0.203	0.172	118.8	10.69	5.2	0.85	0.054	0.065	0.012	0.013

dizer, tests C8 and C9. The effect of gap height was investigated by increasing the gap height and oxidizer flow rate proportionately to maintain the same mass flux in tests C10 and C11. Test C12 had twice the baseline gap height while maintaining the baseline oxidizer mass flow rate yielding half the initial mass flux. The effect of chamber pressure was investigated with test C13, where the chamber pressure was roughly twice baseline. The effect of inlet geometry at the entrance to the radial flow port was investigated by firing a grain with a 45-deg bevel in the hole of the upper fuel disk, test C14.

The *OF* ratio based on total expelled propellant masses varied from 3.9 to 5.2. While this is substantially below the optimal *OF* near 7.5 for this propellant combination, a significant amount of fuel was consumed in the nozzle entry regions. In a more efficient (but more costly) design, this region would be lined with ablative insulators to provide a mixing/postcombustion volume prior to nozzle entry. We presume that this factor (fuel combustion near nozzle entry) also had some effect on the c^* efficiency values that ranged from 83 to 95% in the units tested.

Finally, we note that the average oxidizer flux levels are fairly low when compared with conventional axial flow designs. These low values were a result of the self-imposed limit on a mass flux of approximately 0.5 lbm/in.^{2} s at ignition in the entrance to the radial flow section. For the small-scale apparatus used in these tests, a substantial shift in mass flux occurs as a result of radial variation in the port area and significant regression relative to port gap height. Presumably, full-scale devices may want to employ a similar design philosophy to maximize volumetric efficiency by starting with a gap height much smaller than the web distance burned.

General Fuel Regression Behavior

A digitally captured photograph of a representative postfire fuel grain that illustrates the nature of the regression is provided in Fig. 4. Based on the expected flow characteristics illustrated in Fig. 2a, an argument can be made to explain the regression trends that can also be correlated to the surface patterns seen on the postfired fuel grains. The upper disk is characterized by a star-shaped pattern in which the interior portion contains char-like deposits, and the outer portion is smoother. It is possible that the region with the char deposits is indicative of a low regression rate area in which fuel depolymerization has taken place because of the relatively thick melt layers that would be present under these conditions. Another explanation may attribute the rough, blackened zone to a turbulent region, with relaminarization occurring in the smooth regions near nozzle entry points.

The lower fuel disk shows substantial fuel removal near the nozzles, as well as a circumferential groove that extends between nozzles. The grooves could be explained by the presence of a steady vortex ring in this location. Many lower fuel disks also tend to exhibit plateau structures near the centerline—substantial deposition of upstream material and motion of the melt layer might explain this appearance. On average, the fuel

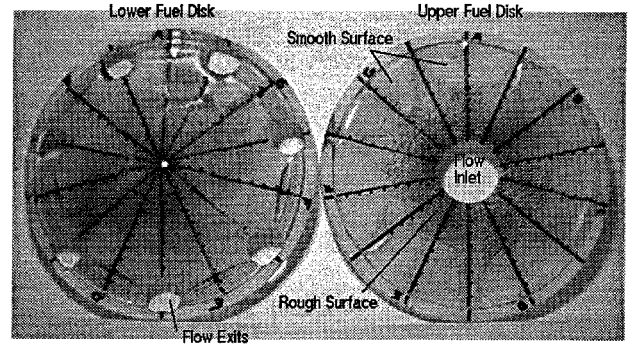

Fig. 4 Post-fire fuel grain (test C11).

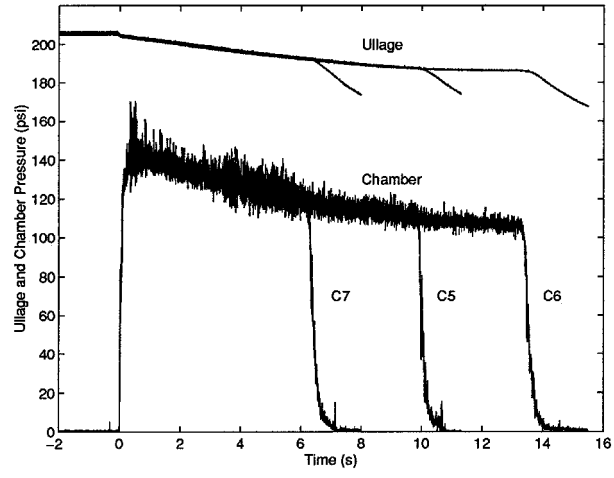

Fig. 5 Chamber and ullage pressure histories, tests C5, C6, and C7.

regression rates were much higher than expected for the flux levels tested. For example, in test C5, we estimate average regression rates on upper and lower plates of 0.014 and 0.017 in./s, respectively at an average total flux of 0.059 lbm/in.^{2} s (see Table 1). Previous correlations from axial-flow tests[11] predict a regression rate of 0.0056 in./s at this flux and pressure level; about one-third that experienced in the radial-flow test.

Time History Series

The first three tests started with the same geometry and were fired for 6.3, 9.9 and 13.4 s, respectively. The longest test experienced burn-through on the lower plate, which caused it to lift off the aft flange with some evidence of regression on the back side of the fuel disk. The ullage and chamber pressure traces for these tests are overlaid in Fig. 5. Note the reproducibility of the chamber pressures, particularly in the range from 0 to 6.3 s, where all three tests agree well within the magnitude of the combustion oscillation. The large amplitude oscillation seen at roughly 5 s may be related to the expulsion

of the phenolic inserts in the aft fuel disk. The oscillation in the steady-state mode is on the order of ±5% of the chamber pressure.

A sample of the postfire fuel measurements is provided to give some idea of the azimuthal variations by plotting the disk thicknesses along the 14 different rays in Fig. 6. The azimuthal variation is modest with the exception of the impingement region on the lower plate. The azimuthally averaged surface geometry for both prefire and postfire conditions of the three time history tests are shown in Fig. 7. On the upper fuel disk, overall surface recession is smallest near the radial entry point (particularly on the longer duration tests), and becomes quite uniform at outboard locations. This behavior might be explained by the presence of a separation region between the corner and the 1.25-in. radial location.

The lower disk is characterized by stagnation point heat-transfer behavior (as in Fig. 2b) near the radial entry point where peak recession presumably occurs near the edge of the impinging jet. This is seen at the 0.75-in. radial station in Fig. 7. The outboard recession (radial locations beyond 1.0 in.) exhibits a slight variation with increased radius. Here we note that the theoretical behavior (assuming a regression law of the form $r = aG_{ox}^{0.8}$) would predict the recession to vary radially as $R^{-0.8}$. The recession on the outboard regions of both disks in Fig. 7 show a much weaker variation than this theory would suggest indicating a much weaker dependence on radial location. This is a positive result, because it indicates the possibility of developing a device with relatively uniform regression for outboard radial stations where the bulk of the fuel surface lies.

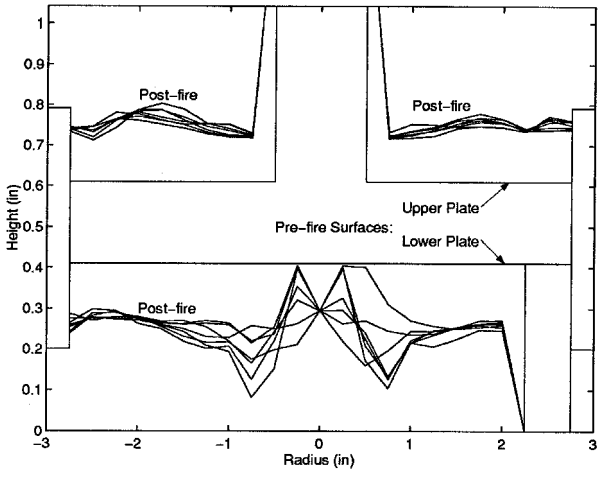

Fig. 6 Azimuthal variation in surface regression, test C5.

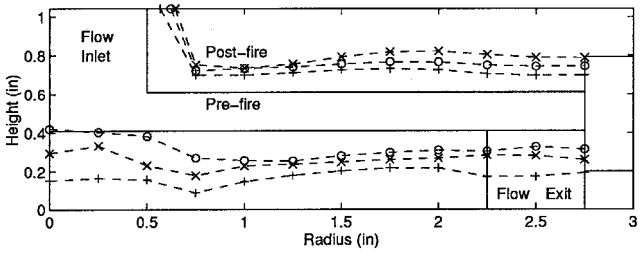

Fig. 7 Azimuthally averaged geometry (prefire and postfire) for tests C6 (○), C5 (×), and C7 (+).

The radial variation in the regression rate for the upper and lower disks is shown in Fig. 8 for this test series. The regression behavior of the lower disk shows the jet ring peak at 0.75-in. radius, except for the short test. It seems that the impingement behavior takes some time to develop, other short duration tests also show the behavior of C7. Outboard of this peak, regression rates are reduced corresponding to the decrease in mass flux as a result of increasing port area. Surprisingly, as the radius increases, decreasing the net flux, the regression rate on the upper plate is seen to increase from the 0.75- to 1.75-in. radial locations. After the 1.75-in. radial location, the regression rate of the upper and lower disks are relatively close. This seems to confirm the supposition that the flow is attached on both disks. The regression rates on the upper and lower disks merge by the 1.75- or 2.0-in. radial station for all tests but C12, where separation may persist further and C14 where the separation is presumably smaller.

Effect of Mass Flux on Regression Rate

The baseline geometry was tested at time-averaged oxidizer mass flow rates of 0.159, 0.245 and 0.307 lbm/s. These correspond to initial inlet oxidizer mass fluxes of 0.253, 0.390, and 0.489 lbm/in.^{2} s. To match the chamber pressure, the ullage pressure and nozzle throat diameters were increased accordingly to maintain the same pressure differential across the injector. The burn time decreased with increasing oxidizer mass flow rate because the same volume of fluid was loaded for each test. The combination of enhanced burning during the ignition phase, short burn times, and the fact that the fuel regression rate increased with increasing flux led to increased average chamber pressures for tests C8 and C9.

The radial variation in the regression rate on the upper and lower fuel disks for the mass flux test series is plotted in Fig. 9. The effect of increasing the flux was to increase the local regression rate on both the upper and lower fuel disks. The presence of the jet ring peak regression on the lower disk is not apparent in tests C8 and C9, which are shorter duration than C5. This is believed to be caused by fuel deposits that may occur during the ignition phase. The trend of seeing in-

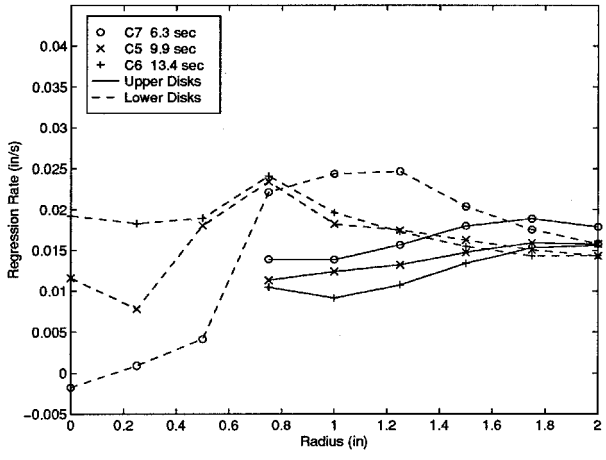

Fig. 8 Regression rate variations with time.

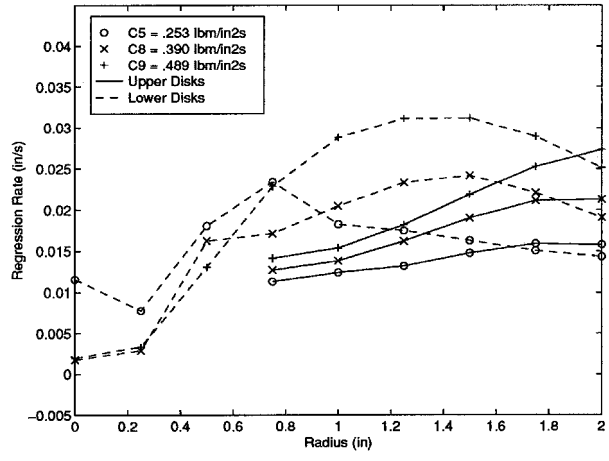

Fig. 9 Effect of mass flux level on fuel regression rates.

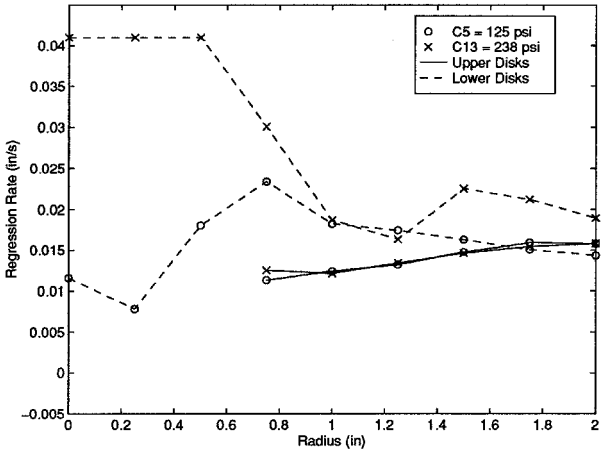

Fig. 10 Effect of chamber pressure on regression rates.

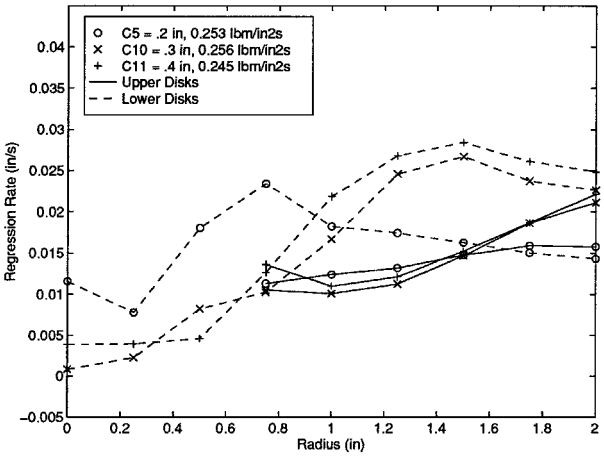

Fig. 11 Effect of initial gap height on regression rates.

creased regression with radial station is seen again between the 0.75- and 2-in. radius. On the upper disk, the peak regression occurs at 1.75 in. for the low flux case and moves over to 2 in. for the higher flux cases. This movement is believed to be associated with the reattachment point of the recirculation region moving. This trend is not corroborated by the lower fuel disks (though they are adversely affected by the impingement behavior). The jet ring erosion is not seen because of a short burn time, which makes it more susceptible to fuel deposit during the ignition phase.

Other Parametric Tests

The radial variation of fuel regression for the baseline case and the same geometry run at roughly twice the pressure is plotted in Fig. 10. The pressure effect is negligible on the upper fuel disk. There seems to be a significant pressure effect, not only on the magnitude, but the nature of the regression on the lower fuel disk. Some of this is undoubtedly a result of the difficulty in maintaining consistent ignition behavior and axisymmetry between the tests. However, the area-averaged trend shows conclusively that the regression on the lower surface is enhanced by the pressure; especially in the impingement region. The pressure effect seen in regression may actually be the effect of having a higher mass flux. Additional testing would be required to investigate this phenomena.

No distinct effect of gap height on regression rate at the same flux level and chamber pressure is seen in Fig. 11. The similarities between tests C10 and C11 on both the upper and lower plates and how they differ from C5 suggest that the overall behavior is extremely dependent on the nature of the impingement behavior in the center of the lower disk. Both Figs. 10 and 11 support the idea that the nature of regression on the upper fuel disk, controlled by the structure of the flow, is a function of mass flux.

Conclusions

Experimental studies involving a center-injection, radial-flow hybrid rocket have confirmed that such a device can support ignition and stable combustion. While the theoretical tendency is to have surface regression drop as $R^{-0.8}$, measurements indicated a much weaker radial variation. The recession was reasonably uniform azimuthally, with the exception of the impingement region on the lower disk. These results are encouraging, because practical designs with good fuel utilization appear to be feasible. Detailed regression on both upper and lower fuel disks is very complex, being influenced by flow separation, flow impingement (on the lower disk), and numerous three-dimensional effects. On average, the regression rates were not as great on the upper disk as those on the lower disk, but both rates were greater than that observed in a conventional axial-flow hybrid at the same initial flux and chamber pressure levels.

References

[1]Boardman, T., Carpenter, R. L., Goldberg, B. E., and Schaeffer, C. W., "Testing and Development of 24-in Hybrid Motors Under the Joint Government/Industry IR&D Program," AIAA Paper 94-3019, June 1994.

[2]Caravella, J. R., Jr., "Experimental Investigation of Combustion in a Radial Flow Hybrid Rocket Engine," M.S. Thesis, Purdue Univ., West Lafayette, IN, Aug. 1996.

[3]Moller, P. S., "Radial Flow Without Swirl between Parallel Discs," *The Aeronautical Quarterly*, Vol. 14, May 1963, pp. 163–186.

[4]Raal, J. D., "Radial Source Flow Between Parallel Disks," *Journal of Fluid Mechanics*, Vol. 85, Pt. 3, 1978, pp. 401–416.

[5]Prata, A. T., Pilichi, C. D. M., and Ferreira, R. T. S., "Local Heat Transfer in Axially Feeding Radial Flow Between Parallel Disks," *Journal of Heat Transfer*, Vol. 117, Feb. 1995, pp. 47–53.

[6]Mochizuki et al., "Heat Transfer Mechanisms and Performance in Multiple Parallel Disk Assemblies," *Journal of Heat Transfer*, Vol. 105, Aug. 1983, pp. 598–604.

[7]Mochizuki, S., and Yang, W.-J., "Self-Sustaining Radial Oscillating Flows Between Parallel Disks," *Journal of Fluid Mechanics*, Vol. 154, 1985, pp. 377–397.

[8]Mochizuki, S., and Yang, W.-J., "Local Heat-Transfer Performance and Mechanisms in Radial Flow Between Parallel Disks," *Journal of Thermophysics and Heat Transfer*, Vol. 1, No. 2, 1987, pp. 112–116.

[9]Wernimont, E. J., and Heister, S. D., "Performance Characterization of Hybrid Rockets Using Hydrogen Peroxide Oxidizer," AIAA Paper 95-3084, July 1995.

[10]Gordon, S., and McBride, B. J., "Computer Program for Calculation of Complex Chemical Equilibrium Compositions, Rocket Performance, Incident and Reflected Shocks; and Chapman-Jouguet Detonations," NASA SP-273, 1971.

[11]Wernimont, E. J., and Heister, S. D., "Progress in Hydrogen Peroxide Oxidized Hybrid Rocket Experiments," AIAA Paper 96-2696, 1996.